Perceptual decision making: Biases in post-error reaction times explained by attractor network dynamics

Kevin Berlemont, Jean-Pierre Nadal

Perceptual decision making: Biases in post-error reaction times explained by attractor network dynamics

Kevin Berlemont[1], **and Jean-Pierre Nadal**[1, 2]

[1] Laboratoire de Physique Statistique, École Normale Supérieure, PSL University, Université Paris Diderot, Université Sorbonne Paris Cité, Sorbonne Université, CNRS, 75005 Paris, France.

[2] Centre d'Analyse et de Mathématique Sociales, École des Hautes Études en Sciences Sociales, PSL University, CNRS, 75006 Paris, France.

Keywords: perceptual decision making, reaction times, attractor networks, post-error slowing.

Abstract Perceptual decision making is the subject of many experimental and theoretical studies. Whereas most modeling analysis are based on statistical processes of accumulation of evidence, less attention is being devoted to the modeling with attractor network dynamics, even though they describe well psychophysical and neurophysiological data. In particular, very few works confront attractor models predictions with

data from continuous sequences of trials. Recently however, a biophysical competitive attractor network model has been used to describe such sequences of decision trials, and has been shown to reproduce repetition biases observed in perceptual decision experiments. Here we propose an extension of the reduced attractor network model of Wong and Wang (2006) to get more insights into such effects. We make explicit the conditions under which such network can perform a succession of decisions, and show that the model provides a mathematical framework for studying the effects of a trial on the decision made on the next one. We study in details the reaction times properties during a sequence of decision trials, and show that the model reproduces behavioral data, both qualitatively and quantitatively. In particular, we find that the decision made on the current trial is biased toward the one made on the previous trial. More remarkably, we show that, in the absence of any feedback about the correctness of the decision, the network exhibits post-error slowing, a subtle effect in agreement with empirical data.

1 Introduction

Typical experiments on perceptual decision making consists in series of successive trials separated by a short time interval, in which performance in identification and reaction times are measured. The most studied protocol is the one of Two-Alternative Forced-Choice (TAFC) Task – see e.g. Laming (1979b); Vickers (1979); Ratcliff (1978); Usher and McClelland (2001); Shadlen and Newsome (1996); Link and Heath (1975); Townsend and Ashby (1983); Ratcliff (2004); Busemayer and Townsend (1993). Most theoretical studies of reaction times are based on biased random walks/accumulator

models or drift diffusion models (DDM) – see e.g. Ratcliff (1978); Ashby (1983); Shadlen et al. (2006); Ratcliff and McKoon (2008); Bogacz (2009)–, which implement the idea of stochastic integration of input signals until a decision threshold is reached. Despite the fact that the concept of time integration in decision making is appealing, and allows to account for a wide variety of experimental results, it is not obvious how those decision mechanisms are represented in the brain, and what types of choice behavior engage such process (Uchida and Mainen, 2003). An alternative modeling approach has been proposed by Wang (2002), based on a biophysically detailed cortical network model of interconnected leaky integrate-and-fire (LIF) neurons. The model is shown to account for the random dot experiments results of Shadlen and Newsome (2001) and Roitman and Shadlen (2002). In those experiments, a monkey performs a motion discrimination task, in which it needs to decide whether a motion direction, embedded into a random dot motion, is towards left or right. In contrast with drift-diffusion models, mathematical analysis cannot be performed for such complex networks, and one must rely on simulations. However, in Wong and Wang (2006), the authors propose a reduced winner-take-all model obtained by a systematic reduction of the detailed biophysical attractor network model of Wang (2002). Within a mean-field approach, the reduced model consists in an effective network of only two variables, representing the pool activities of two populations of cells, each one being specific to one direction of orientation or the other. All along the reduction from the full model to the one with two units, equations are derived and parameters values are chosen in order to preserve as much as possible the dynamical and behavioral properties of the original full model. Thanks to this reduction, it is then possible to perform a detailed mathematical analy-

sis. In particular, the networks dynamics can conveniently be represented in a 2-d phase plane, and a bifurcation diagram can be drawn.

This decision-making attractor network model has been studied in a context where one goal is to keep in memory the previous decision. This working memory effect is precisely achieved by having the network activity trapped into an attractor state. However, this effect is too strong. If the model is to be used for a series of consecutive trials, the neural activities have to be reset in the neutral state before the onset of the next stimulus. Otherwise, without ad-hoc resetting, only unrealistically strong inputs allow for leaving the current attractor and thus for making a different decision. A more complex network has been proposed by Lo and Wang (2006) in order to account for the control of the decision threshold, with a mechanism which induces a resetting of the activities just after decision. However, the behavior of this model has not been studied in the context of sequences of trials.

Indeed, in behavioral experiments, subjects perform sessions composed of a continuous series of trials, and recent studies have demonstrated strong serial dependence in perceptual decisions between temporally close stimuli (Fecteau and Munoz, 2003). Those previous trial effects are various and several hypothesis on their origin have been discussed: they might be the consequences of attention, competing motor programs (McPeek et al., 2000), guessing strategies, maintaining or switching, priming or procedural learning (Tipper (2001); Gupta and Cohen (2002)). This serial dependence in perceptual decision making has been theoretically studied in the framework of drift diffusion models (Dutilh et al., 2011), or with biasing mechanisms explicitly implemented in the architecture of a complex dynamical network (Gao et al., 2009). The

issue of dealing with such continuous sessions in attractor network models has been recently approached in Bonaiuto et al. (2016). For this, the authors consider a variant of the detailed biophysical model of Wang (2002) in which the working memory phase is suppressed (as we will explain later). The main result is that the performance of the network is, as one would expect, biased toward the previous decision, an effect which decreases with the inter-trials time. However, for short inter-trial times (less then 1 second), this model version remains unable to perform sequential decision-making, and thus this issue needs to be revisited.

The purpose of this paper is to reconsider the attractor network approach of Wang (2002) in the context of successive trials, taking advantage of the reduced model version of Wong and Wang (2006) which allows for a detailed analysis. We first discuss the reduced model behavior in that context of sequential decision tasks. Then, in line with Lo and Wang (2006) who take into account a coupling with the basal ganglia, we propose a biophysically motivated variant of the reduced model and show that it allows to deal with sequences of trials. Then we explore the serial dependence effects predicted by the model and compare with empirical findings. Beside the expected decision bias toward the previous decision, we find that, without any fine tuning of parameters, the model reproduces the post-error slowing (PES) effect: in the absence of feedback on the correctness of the decision, reaction time tends to be longer for the trial following a trial with incorrect decision.

This paper is organized as follows. In a first section we introduce the neural network of Wong and Wang (2006), and we augment it in order to perform sequential decision-making. Predictions of the model on sequential effects are then described and

qualitatively compared to experimental results. The effects of repetition/alternation, as well as the post-error/success effects, are explored. We focus on effects on reaction times and on a dynamical explanation for those effects, but briefly address the effects of error trials on performance. Finally we note some open questions, and comment on some aspects of the model.

2 Methods

In this section we first recall (subsection 2.1) the reduced attractor network model of Wong and Wang (2006). Then, in subsection 2.2, we introduce the extension of this model, obtained by adding an inhibitory current mimicking an input from the basal-ganglia onto the decision units, showing that it allows to deal with sequences of decision trials.

2.1 A reduced recurrent network model for decision-making.

We consider here the reduced attractor network model derived in Wong and Wang (2006), whose architecture is illustrated on Figure 1.A. Two competing units, each one representing a neuronal pool, are selective to one direction of orientation or the other. The decision process is linked to the dynamics of the network. It corresponds to a transition from an initial state, where both units fire at low rates, to a decision state where one is firing at a higher rate (winner) and the other at a lower rate (loser) (Figure 1.B).

In the model there are excitatory and inhibitory couplings between the two populations. Each unit inhibits each other, while they perform self-excitation. The model

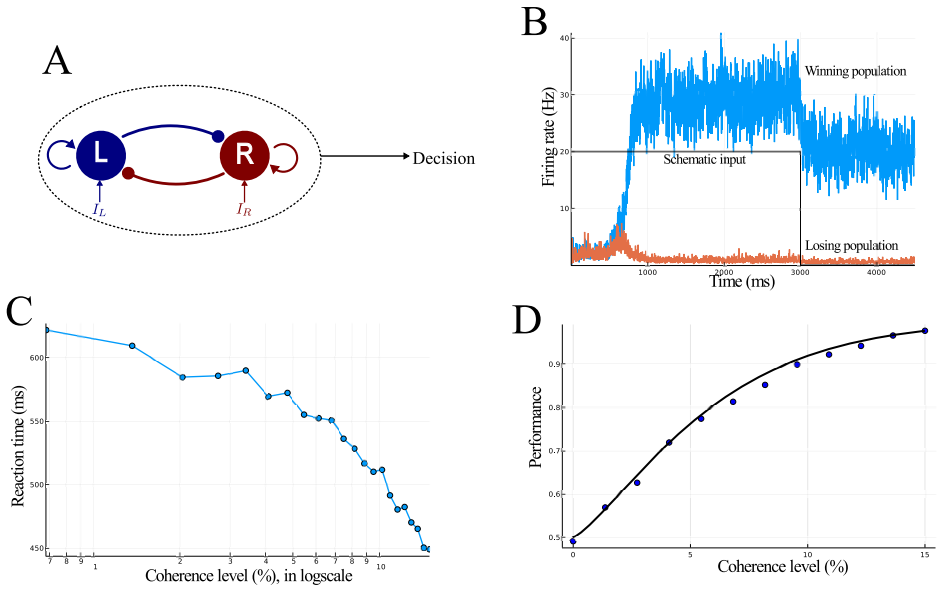

Figure 1: **Wong and Wang two-variable model.** *(A) Reduced two-variable model constituted of two neural units, endowed with self-excitation and effective mutual inhibition. (B) Time course of the two neural activities during a decision-making task. At the beginning the two firing rates are indistinguishable. The firing rate that ramps upward (blue) represents the winning population, the orange one the losing population. A decision is made when one of the firing rate crosses the threshold of* 20 *Hz. The black line represents the duration of the selective input corresponding to the duration of accumulation of evidence until the decision threshold is reached. This model shows working memory through the persistent activity in the network after the decision is made. Panels (C) and (D), Model simulations on one virtual subject: (C) Mean reaction time in the decision task, and, (D) Performance, both in function of stimulus coherence (stimulus ambiguity).*

is described by the following set of dynamical equations (see Appendix of Wong and

Wang (2006)),

$$\frac{\mathrm{d}S_i}{\mathrm{d}t} = -\frac{S_i}{\tau_S} + (1 - S_i)\,\gamma f\,(I_{i,tot}) \tag{1}$$

where S_i is the synaptic drive originating from pool $i \in \{L, R\}$, and $I_{i,tot}$ is the total synaptic current at the population i. The function f is the effective single-cell input-output relation:

$$f\,(I_{i,tot}) = \frac{aI_{i,tot} - b}{1 - \exp\left[-d\,(aI_{i,tot} - b)\right]} \tag{2}$$

where a, b, d are obtained by numerical fit. The total synaptic input currents, taking into account the inhibition between populations, the self-excitation, the background current and the stimulus-selective current can be written as:

$$I_{L,tot} = J_{L,L}S_L - J_{L,R}S_R + I_{stim,L} + I_{noise,L} \tag{3}$$

$$I_{R,tot} = J_{R,R}S_R - J_{R,L}S_L + I_{stim,R} + I_{noise,R} \tag{4}$$

with $J_{i,j}$ the synaptic couplings. The minus signs in the equations make explicit the fact that the inter-units connections are inhibitory (the synaptic parameters $J_{i,j}$ being thus positive or null). The term $I_{stim,i}$ is the stimulus-selective external input. If μ_0 denotes the strength of the signal, the form of this stimulus-selective current is:

$$I_{stim,i} = J_{A,ext}\mu_0 \left(1 \pm \frac{c}{100\%}\right) \tag{5}$$

with $i = L, R$. The quantity c is the coherence level of the stimulus, the percent of dots contributing to the coherent motion. It gives the strength of the signal bias, positive when the stimulus favors population L, negative in the other case. Following Wang (2002), this input represents activity of middle temporal neurons firing in their preferred directions. This input current is only present during the presentation of the stimulus,

and is shut down once the decision is made. The performance of the network depends strongly on the amount of stimulus-selective current.

In addition to the stimulus-selective part, each unit receives individually an extra noisy input, fluctuating around the mean effective external input I_0:

$$\tau_{noise}\frac{\mathrm{d}I_{noise,i}}{\mathrm{d}t} = -\left(I_{noise,i}(t) - I_0\right) + \eta_i(t)\sqrt{\tau_{noise}}\sigma_{noise} \tag{6}$$

with τ_{noise} a synaptic time constant which filter the white-noise. Unless otherwise stated, parameters values will be those of Table 1.

Parameter	**Value**	**Parameter**	**Value**
a	270 Hz/nA	σ_{noise}	0.02 nA
b	108 Hz	τ_{noise}	2 mS
d	0.154 s	I_0	0.3255 nA
γ	0.641	μ_0	30 Hz
τ_S	100 ms	$J_{A,ext}$	5.2×10^{-4} nA. Hz^{-1}
$J_{N,LL} = J_{N,RR}$	0.2609 nA	$J_{N,LR} = J_{N,RL}$	0.0497 nA
θ	20Hz		
$I_{CD,max}$	0.03 nA	τ_{CD}	200ms

Table 1: Numerical values of the model parameters: above the dashed line, as taken from Wong and Wang (2006) (except for θ, here $20Hz$ instead of $15Hz$); below the dashed line, values of the additional parameters specific to the present model (see text).

Initially the system is at a symmetric state, with low firing rates and synaptic activities (see Appendix A.1). On the presentation of the stimulus, the system evolves towards one of the attractor states, corresponding to the decision state. In these attractors, one of the units fires at a higher rate than the other. We are interested in reaction time experiment. Hence in our simulations, we consider that the system has made a decision when for the first time the firing rate of one unit crosses a threshold θ, fixed here at 20 Hz. We have chosen this parameter value, slightly different from the one in Wong and Wang (2006), from the calibration of the extended model discussed below on sequential decision trials with short response-stimulus intervals, of a few millisecond.

2.2 Model extension: Post response dynamics.

As recognized by Wong and Wang (2006), in its original form the model does not capture effects of previous trials on the performance of the present trial. Actually, this recurrent network is not able to perform sequences of decision-making without any modification. Indeed the decision state consists in being in one attractor state (Fig 1B), which is thus the initial state for the next trial. If the next decision has to be the opposite one, exiting the attractor, in order to reach the other one, would require an input with an unrealistically strong bias.

Studies like Roitman and Shadlen (2002) show that, during decision tasks, neurons activity experience a decay following the responses. The prefrontal cortex-basal ganglia-thalamic circuit (BG) plays a fundamental role in many cognitive functions including perceptual decision-making (see Wei et al. (2015)), inhibitory control and working memory. The BG circuit has been studied as providing a mechanism for modulating

the decision threshold in reaction time tasks in Lo and Wang (2006). The authors introduce an extension of the biophysical model of Wang (2002) consisting in modeling the coupling between the network, the basal ganglia and the superior colliculus. The net effect is an inhibition onto the populations in charge of making the decision. The authors show that the decision threshold is signaled by an all-or-none inhibitory burst response towards the cortical neurons, a corollary discharge (CD). The issue addressed in Lo and Wang (2006) is the control of the decision threshold. However, the relaxation itself induced by the corollary discharge, and the effect on sequential decision tasks, are not discussed.

In order to study these sequential effects, we focus on the analysis of the reduced attractor network. We thus modify the reduced model assuming that, after crossing the threshold, the network receives an inhibitory current, mimicking the joint effect of basal-ganglia and superior colliculus on the two neural populations (Figure 2). The

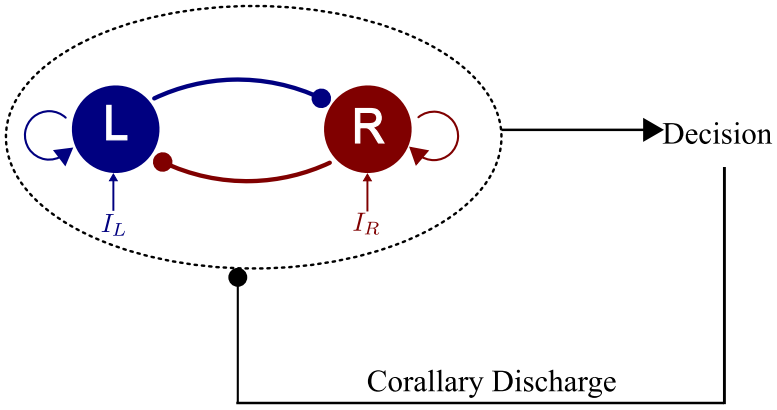

Figure 2: **Schematic extended two-variable model.** *The network consists of two units as in the original model, with mutual inhibition and self-excitation. The extension consists in the addition of the corollary discharge originating from the basal ganglia, an inhibitory input onto both units occurring just after a decision is made.*

form of this corollary discharge is taken with a standard exponential form (Finkel and Redman, 1983):

$$I_{CD}(t) = -I_{CD,max} \exp(-t/\tau_{CD}) \tag{7}$$

with $t = 0$ corresponding here to the time of the decision (or threshold-crossing in our case). The relaxation time constant is chosen in the biological range of synaptic relaxation times and in accordance with the relaxation-times range of the attractor (see Appendix A.2), $\tau_{CD} = 200$ ms. Therefore the input currents are modified as follows:

$$I_{L,tot}(t) = J_{LL}S_L(t) - J_{L,R}S_R(t) + I_{stim,L}(t) + I_{noise,L}(t) + I_{CD}(t) \tag{8}$$

$$I_{R,tot}(t) = J_{RR}S_R(t) - J_{R,L}S_L(t) + I_{stim,R}(t) + I_{noise,R}(t) + I_{CD}(t) \tag{9}$$

where the current $I_{CD}(t)$, corresponding to the inhibitory input originating from the basal ganglia, is given by:

$$I_{CD}(t) = \begin{cases} 0 & \text{during stimulus presentation} \\ -I_{CD,max} \exp\left(-(t - t_D)/\tau_{CD}\right) & \text{after the decision time, } t_D \end{cases} \tag{10}$$

If the inhibitory current following the decision is too weak, the network behaves as in the absence of this current, that is, it is not able to make a new decision different from the previous one (Figure 3.A). Even when the opposite stimulus is presented, the system cannot leave the attractor previously reached, unless in presence of unrealistic strong biases. If however the strength I_{BG} is strong enough, the corollary discharge allows the system to relax towards a resting state between stimuli, hence to perform sequential decision making tasks (Figure 3.B). The behavior of this model variant can be analyzed making use of non-linear dynamical tools. Figure 4 illustrates how the corollary discharge following a response modifies the energy landscape (potential well in which the system evolves) with respect to the original model.

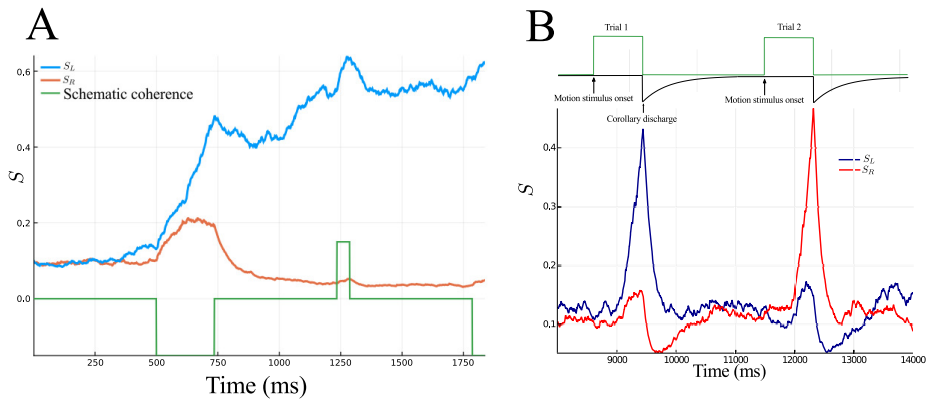

Figure 3: **Time course of synaptic activities for the modified and the control network.** *(A) The green curve represents, schematically, the onset of the stimulus with the sign of the bias (coherence). In this simulation,* $I_{CD,max} = 0.01$ *nA and the model is not able to perform sequential decision-making. The blue and orange curve correspond to the activity of the units. During the resting time, the previous attractor state is not leaved. (B) The upper part corresponds to a schematic time course of the input signal and of the control one. The input signal (green) corresponds to the sensory information acquired during the task, and the control signal (black) to the corollary discharge from basal ganglia towards the network. Here, we take* $I_{CD,max} = 0.03$ *nA. The lower part represents the time course of the neural activities* S_L *and* S_R *in the model. The first stimulus leads to the choice* R*, and we observe the decay following response. This allows the network to make the opposite choice,* L*, for the second stimulus.*

Without any inhibitory current, during the inter-trial time, the network will stay in the current attractor state. Hence the next trial will be strongly biased and the network will not be able to change its state without a strong coherence input. With the inhibitory corollary discharge, the network relaxes towards a new attractor state, with lower firing rates. After the threshold is crossed by the one of the two neural populations, there is big drop in the activity. This corresponds to the exit of the attractor state by the system. This type of time-course is in agreement with the experimental findings of Roitman and Shadlen (2002) who measure the activity of LIP neurons during a decision task. During the resting time, the amount by which the activities decay influences the following trial by changing the initial condition before the new stimulus arrives.

3 Results

3.1 Sequential dynamics and choice repetition biases

As just explained, the extended model is able to perform sequential decision-making during a continuous session. We now test if we recover the main sequential effects observed in behavioral experiments. We first address the question of response repetition bias, as studied in Bonaiuto et al. (2016). The effect of the previous trial choice impacts the next one for short response-stimulus intervals (RSI). The RSI is the time between the response of the subject and the presentation of the next stimulus. For details about the simulations, or the statistical tests, see Appendix A.1.

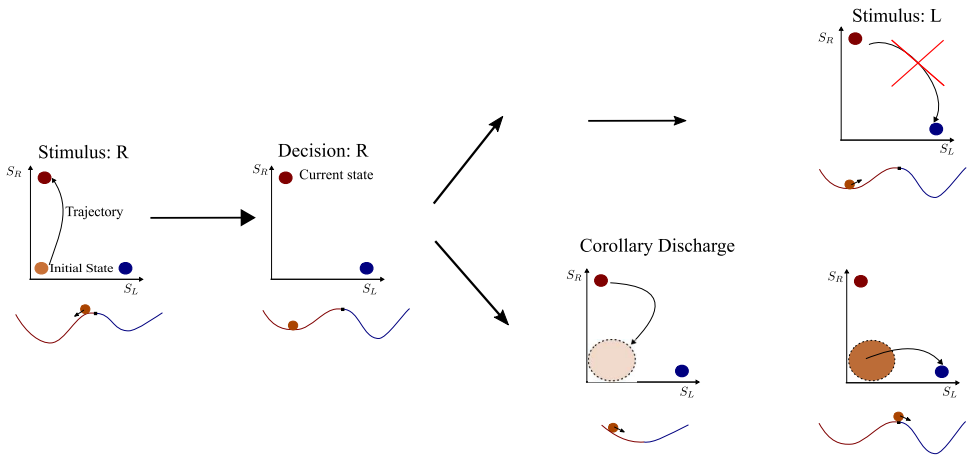

Figure 4: **Phase-plane analysis of the sequential decision making:** *Schematic representation of the neural dynamics in the phase-plane, and the corresponding energy landscape, when performing sequential decision-making. The red color correspond to the attractor R, and the blue to attractor L. The first two schema are identical for the two models because the way they perform decision is the same. We describe the behavior of the original model (Wong and Wang, 2006), between two consecutive stimuli, in the upper panel , and the one of our model in the second panel.*

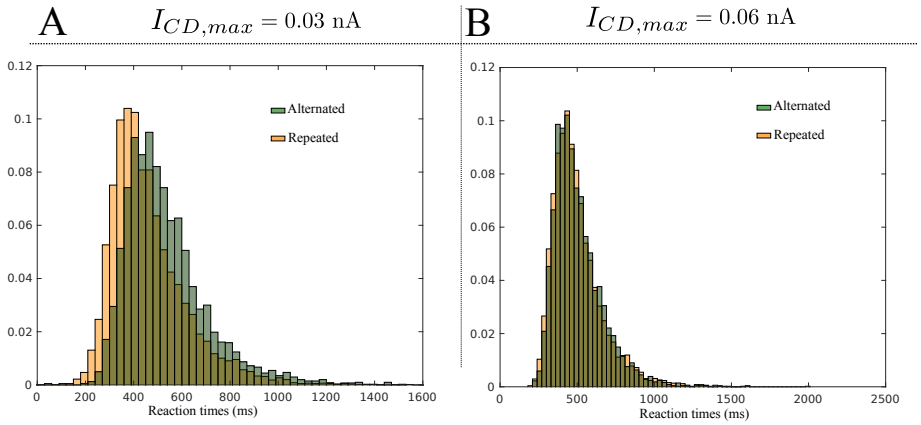

Figure 5: **Histogram of the reaction times.** *The simulations were run at (A)* $I_{CD,max} = 0.03$ *nA and (B)* $I_{CD,max} = 0.06$ *nA, with a RSI of* 1.5 *second. The green histogram corresponds to the Alternated case, that is when the decisions made at the* n*th and* n*th* $+1$ *trials are different. The orange histogram corresponds to the Repeated case, that is when the decisions made at the* n*th and* n*th* $+1$ *trials are identical.*

Reaction times biases

We run a simulation on 10000 continuous trials, each of them with a coherence value randomly chosen between 12 values in the range $[-20, 20]$. We analyzed the effect of response repetition by separating the trials in two groups depending on whether the decisions made on the previous and on the current trials are identical or different (*Alternated*: The two decisions are not the same. *Repeated*: The choice is identical to the previous one). We studied the reaction times in those two groups (Figure 5) for two values of the corollary discharge amplitude, $I_{CD,max} = 0.03$ nA and $I_{CD,max} = 0.06$ nA.

We find that in the case $I_{CD,max} = 0.03$ nA, the two reaction-time distributions are different (Smirnov-Kolgomorov test, $p = 2 \times 10^{-97}$), whereas for $I_{CD,max} = 0.06$ nA they are the same (Smirnov-Kolgomorov test, $p = 0.079$). In the regime where those

distributions are different, when the choice is repeated the reaction time is faster (Figure 5A), which means that the behavior of the network is influenced by the previous trial. However if the corollary discharge is strong enough (Figure 5.B), or the RSI too long (Figure 8), one does not observe this effect anymore. Those two parameters can be seen as tuning parameters of this sequential effect. Depending on their value we can observe three different behaviors: the network is not able to leave the current attractor state / the network can escape from the current basin of attraction / the continuous session becomes analog to a series of individual ones with full resetting of the activities between each trial. The range of values of the RSI for which we observe a sequential effect is in accordance with psychological experiments (Laming, 1979b; Rabbitt and Rodgers, 1977) (up to several seconds), and the order of magnitude of the corollary discharge amplitude is similar to the one in more biophysical models of decision-making (Lo and Wang, 2006).

Dynamics analysis

With the relaxation of the activities induced by the corollary discharge, the state of the network at the presentation of the next stimulus thus lies in between the attractor state corresponding to the previous decision, and the neutral attractor state. We find that the relaxation of the network activity, from the previous decision until the onset of the next stimulus, has different behaviors, depending on whether the next decision is identical or different from the previous one (Figure 6). Note that this is a statistical effect which can only be seen by averaging over a very large number of trials.

Figure 6 compares two examples of network activity, one with a alternated choice,

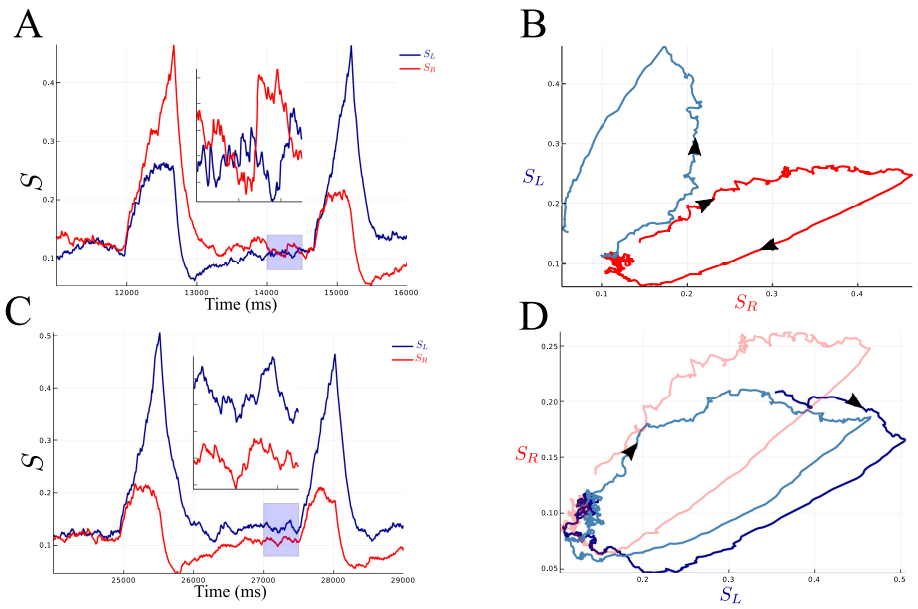

Figure 6: **Decaying tail activity.** *Panels (A) and (B) represent the alternated case where the decision made is R then L, and panels (C) and (D) represent the case where decision L is made and repeated. Panels (A) and (C) plot the time course activities of the network. The light blue zone is zoomed in order to better see the dynamics just before the onset of the second stimulus. The red and blue curves correspond to the activities of, respectively, the R and L network units. Panels (B) and (D) represent, respectively, the (A) and (C) dynamics in the phase-plane coordinates. In order to compare the alternated and repeated cases, (A,B) and (C, D), the dark red curve of panel (B), in coordinates S_R, S_L, is reproduced on panel (D) in the switched coordinates S_L, S_R, giving the light red curve.*

and one with a repeated choice, plotting the dynamics during two consecutive trials. We observe on Figure 6.A, the alternated case, that previous to the onset of the new stimulus (light blue rectangle) the activities of the two populations are at very similar levels. In contrast, for the case of a repeated choice, Figure 6.C, the activities are well separated, with higher firing rates. The simple attractor network architecture allows to make use of tools from dynamical systems in order to study the behavior of the system. Figure 6.B and D represent the dynamic of the network in the phase-plane diagram. As seen on the Figure 6.D, the network states at the time of decision are different depending on whether a same or a different choice is made as compared to the previous trial.

We further develop the analysis of this decaying activity by comparing the relaxation activity for the cases of repeated and alternated choices. Figure 6.D shows, in blue, the phase-plane dynamics in repeated choices. In red we represent the dynamic of the first trial of Figure 6.B. We observe that the relaxation between trials is different in the two cases. However, due to the noisy behavior of the network, the statistical significance is not guaranteed. In order to validate this finding, we represent on Figure 7 the mean activities, obtained by averaging over all trials, separately for each group, the alternated and repeated cases, during the RSI. As expected, for small values of $I_{CD,max}$ (like 0.03 nA) the two dynamics are clearly different. This difference diminishes during relaxation, yet at the onset of the next stimulus we can still observe some residues. On the contrary, for larger values of the inhibitory current, the dynamics are almost identical. The choice repetition bias in reaction time, that we observed in the simulations, results from the differences in the decaying activity. For a range of values of RSI and $I_{CD,max}$, the activities of the two units do not recover totally to baseline. Therefore the

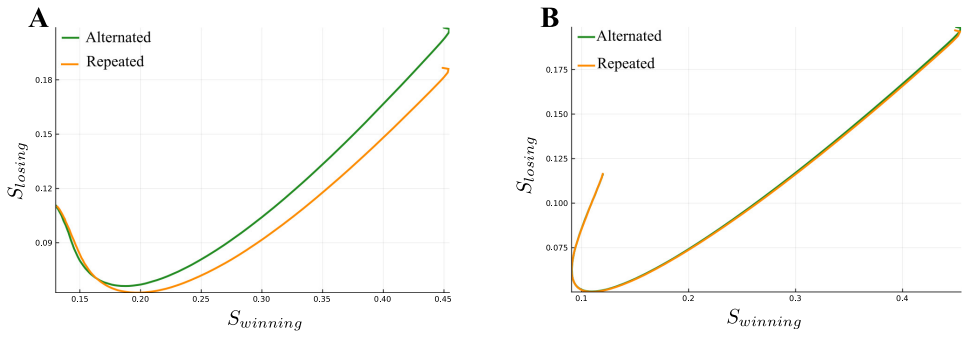

Figure 7: **Phase plane analysis.** *Dynamics of the decaying activity between two successive trials, (A) for $I_{CD,max} = 0.03$ nA, and (B) for $I_{CD,max} = 0.06$ nA. The synaptic activity is average over all trials separately for each one of the two groups: alternated (green) and repeated (orange). The axis are $S_{winning}$ and S_{losing} (not S_R and S_L) corresponding to the mean synaptic activity of, respectively, the winning and the losing populations for this trial. Note the difference in scale of the two axes. The time evolution along the curves is from the high values of $S_{winning}$ (top-right) to the low activity values close to the symmetric state.*

next trial will be biased toward the previous response, as proposed in Bonaiuto et al. (2016) and observed in empirical data Dutilh et al. (2011).

Influence of the RSI

As explained before, our analysis of the resting dynamics of the system shows that if the system is able to return to baseline during the RSI we should not be able to observe choice repetition effects. Hence if we increase the RSI, this effect should be reduced because the network has more time to return to equilibrium. Considering a RSI of 5 seconds, Figure 8 represents the histogram of the reaction-time, as well as the phase-

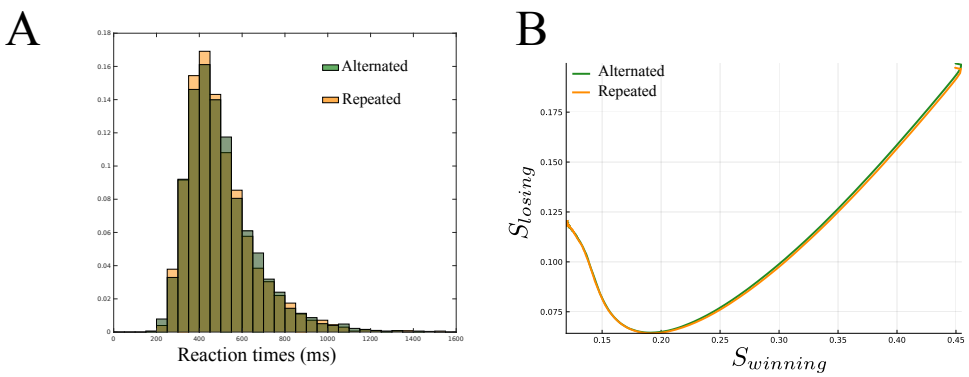

Figure 8: **RSI of** 5 **seconds.** *(A) Histogram of the reaction time for simulations with* $I_{CD,max} = 0.03$ *nA. (B) Average dynamics between two successive trials in the phase-plane coordinates.*

plane dynamics during relaxation.

As expected, with this longer RSI the effect of choice repetition is highly reduced. The distributions of the reaction times of the two groups are essentially identical (Smirnov-Kolmogorov test, fail to reject, $p = 0.019$). Between each stimuli, the network rests near a symmetric fixed point. Because of the longer RSI, the new initial state happens to be closer to the neutral fixed point than for short RSI (Figure 8B). Finally this choice repetition bias in reaction time is explained by the attractor dynamics. The decaying activity depends on the corollary discharge and can influence the next trial. We find the expected result that for longer RSI, the sequence of trials has a reduced effect on the decision. If we consider an even longer RSI, $T = 10$ seconds, we obtain that the reaction times distribution are non distinguishable (Smirnoff-Kolmogorov test, fail to reject, $p = 0.28$).

3.2 Post-error effect

Post-error slowing

In this section we discuss the post-error slowing effect (Laming (1979b), Dutilh et al. (2011)): "The response following an error took significantly longer than an ordinary correct response". We analyze in our model the differences between post-correct trials and post-error trials. By analogy with Laming (1979b), we first consider a sequence of stimuli with two possible coherences (of opposite sign). The sequence is drawn by randomly choosing one value of coherence at each trial.

The first question is whether there is a range of parameters of the model for which one observes post-error slowing, and if the results are coherent with behavioral data. Hence we investigate the model behavior for several values of parameters. On Fig. 9 we represent the mean difference between post-error (PE) and post-correct (PC) reaction times, with respect to the coherence level of the stimuli. Figure 9.A shows the results for a RSI of 500 ms and a inhibitory discharge of 0.035 nA. We observe that the network does exhibit post-error slowing. The gray area on the figure represents the range of coherence level at which this effect is significant. The light blue area represents the standard deviation of the mean on our data. This area is large, and highlight the broad distribution of this effect. However, post-error slowing is a very subtle effect, and reaction times in psychological experiments are known to exhibit a broad distribution (Snodgrass et al., 1967). Hence, those two observations are in accordance which each other.

However this effect does not appear for all values of RSI (Figure 9.B), or of the

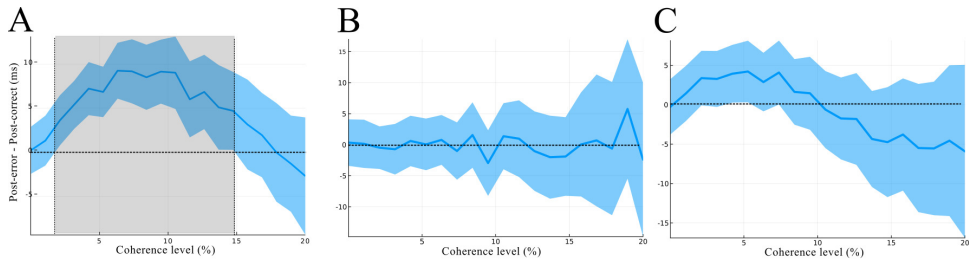

Figure 9: **Post-error slowing.** *Mean post-error reaction times minus post-correct reaction times during sequential decision-making, with respect to coherence levels. (A) The parameters are* $I_{CD,max} = 0.035$ *nA and RSI* $= 500$ *ms. The gray area denotes the region were the curve is highly above the zero-line. (B) and (C): The other parameters are, (B),* $I_{CD,max} = 0.035$ *nA and RSI* $= 5000$ *ms, and (C),* $I_{CD,max} = 0.05$ *nA and RSI* $= 500$ *ms. For each figure, the light blue area denotes the standard deviation of the data.*

corollary discharge (Figure 9.C). For higher values of $I_{CD,max}$, there is a range of coherence levels for which the mean effect of post-error slowing is observed. This effect is weakened by comparison to Figure 9.A, as the curve is closer to the *zero-line*. If we increase the RSI, instead of the inhibitory current, the post-error slowing effect vanishes. The mean value is close to zero for all coherence levels, highlighting the fact that there is no post-error or post-correct differences for those parameters. Finally, a remark is in order. As one increases the coherence level, the standard deviation of this effect increases. This does not come from the fact that the distribution of the post-error effect is broader at large coherence level, but rather that at such high coherence levels, the network almost always answers correctly (Figure 11). Hence there is only a few errors during a sequence, and the post-error slowing is thus harder to observe.

In Figure 10, we zoom on the properties of the post-error effect by presenting the

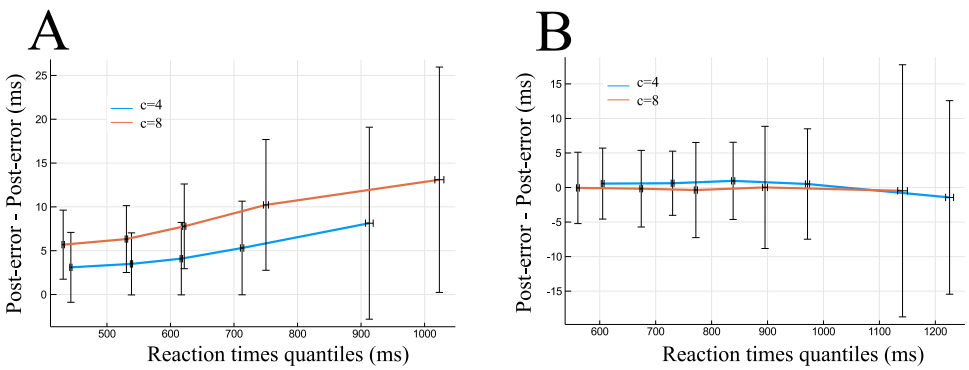

Figure 10: **Delta plots of the PES effect against speed response of the decision.** *(A) The parameters are the following:* $I_{CD,max} = 0.035$ *nA and RSI* $= 500$ *ms. (B) The parameters are the following:* $I_{CD,max} = 0.035$ *nA and RSI* $= 5000$ *ms. For both figures, the effects were obtained by quantile averaged across all simulations. Blue and orange curves are the same quantity at two different coherence levels (* $c = 4$ *for blue and* $c = 8$ *for orange). The error bar represents the standard deviation of the mean on the data. Despite their quite large values (Dutilh et al., 2011), they still reflect some tendency in the behavior of the network.*

data as a delta plot (Speckman et al. (2008), Pratte et al. (2010)). Delta plots allow to show the variable of interest as a function of the response speed. In our case, we average the PES effect during a simulation and we quantile-averaged across several simulations, corresponding to several virtual subjects. By looking at the quantiles of the PES effect we obtain more information than from what can be seen on figure 9. On Figure 10 (short RSI), the global post-error slowing is observed with respect to the response speed of the decision. The delta plot indicates that for slow reaction times the PES is prominent, weaker for faster reaction times. These results are qualitatively similar to the ones of Dutilh et al. (2011) when studying lexical decision data from Keuleers and Brysbaert

(2010). The same analysis for longer RSIs leads to the conclusion that not only the mean PES effect is negligible, but the quantiles are almost identical. Hence the distribution of reaction times for post-correct and post-error trials is globally unchanged for longer RSIs.

Performance following an error

It has longly been observed (Laming (1979b)) that, during a two-alternative-forced-choice experiment, the probability of error following an error trial is modified. We test this effect in our model. We run a simulation with 12 values of coherences, equally distributed between positives and negatives values. We are interested in the proportion of correct responses following an error, independently of the relation between the coherences at the previous trial and the current one. We present the results of these simulations on Figure 11.

The performance following an error is increased compared to the post-correct one (results are analog when comparing to the mean performance on all trials without any distinction) (Figure 11.A). This effect is similar to the one observed in the behavioral experiments of Laming (1979b), where the subject showed increased performance after making an error. One of the first observation is that this effect does not appear at all coherence levels. For low or high values of coherence, the two performances are analog. However for intermediate values, we notice a difference between those quantities at low RSI (500 ms). As for the post-error slowing effect, increasing the RSI leads to the vanishing of this effect (Figure 11.B).

In order to obtain more insights on this effect we studied the discrimination thresh-

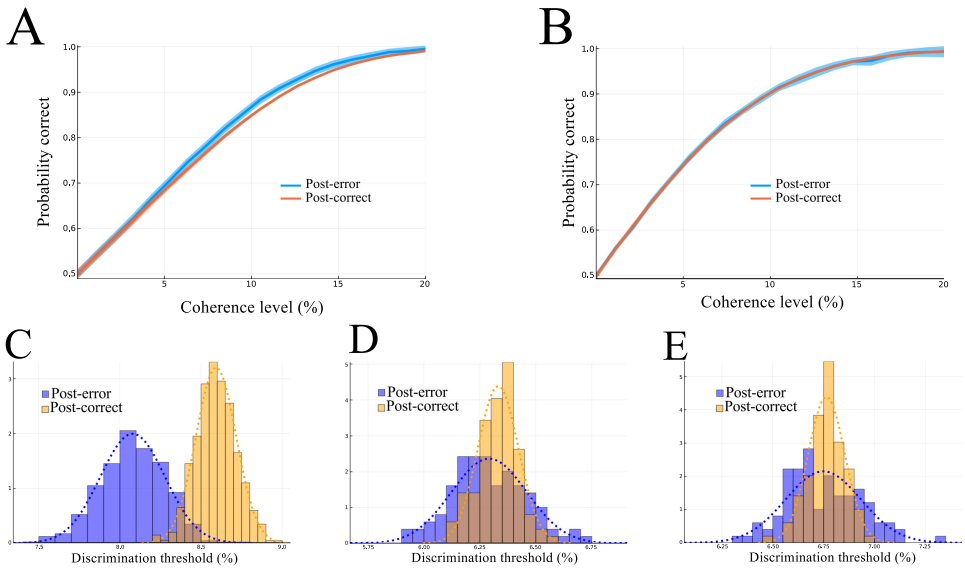

Figure 11: **Performance following an error.** *(A) and (B): Performance of the model during a sequential decision-making task, for a RSI of* 500 *ms (A) and* 5000 *ms (B). In blue, we represent the probability of correct choice following an error with respect to the coherence level, in orange the performance following a success. (C), (D) and (E): Discrimination threshold, at which the performance is* 82% *correct, for a RSI of (C),* 500 *ms , (D)* 1000 *ms and (E)* 5000 *ms. In blue, we plot the distribution of the discrimination threshold following an error and in orange the one following a success. The dashed lines correspond to the fit of the samples by a Normal distribution.*

old following an error, or a success. The definition of the *discrimination threshold* is based on the use of a Weibull function in order to fit the performance of the model (Quick, 1974). The threshold value is chosen as the coherence level at which the subject responds correctly 82% of the time.

For short RSI (Figure 11.C), there is a significant modification of the discrimination threshold between the two conditions: the mean and the variance are changed. The fact that the discrimination threshold is modified characterizes the modification of performance. It highlights the difference between the two conditional probability of choice. In order to apprehend the influence of the RSI on these distributions, we look at the results for higher RSI (Figure 11.D and E). As expected, the higher is the RSI, the closer are these distributions. In particular we observe a displacement of the mean of those distributions toward each other as we increase the RSI. For a RSI of several seconds, Figure 11.B and E, the effect of the error on the performance vanishes.

Dynamical analysis

It is remarkable that the attractor model considered here reproduces the experimental findings: in the absence of external feedback on the correctness of the decision, the reaction times are different depending on whether the decision made at the previous trial was an error or a success. In this section we show that this effect comes from the intrinsic properties of the neural network dynamics.

Figure 12 shows the distributions of the synaptic activities of the losing (panels (A) and (C)), and winning (panels (B) and (D)) populations, at the time of the decision, and this for two RSI values, a short one (panels (A) and (B)) and a large one (panels (C)

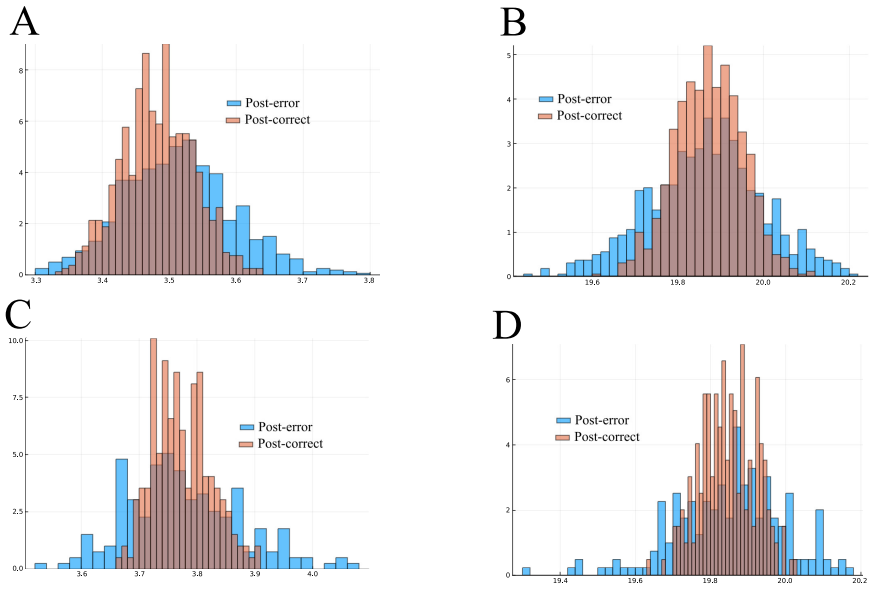

Figure 12: **Dynamical analysis of the post-error trajectory.** *(A) and (C): Distribution of the synaptic activity, at the time of decision, of the losing population. Each histogram represents a different RSI:* 500 *ms for (A) and* 5000 *ms for (C). (B) and (D): Distribution of the synaptic activity, at the time of decision, of the winning population. Each histogram represents a different RSI:* 500 *ms for (B) and* 5000 *ms for (D).*

and (D)). The corollary discharge current being the same for the two populations, at a given RSI value these distributions are closely linked to the relaxation activity, hence to the state just before the onset of the next stimulus. In order to understand the origin of post-error slowing, we analyze these activities conditionally to the correctness, or not, of the previous trial. For the statistical significance (see appendix A.1) of the difference between histograms, we make use of the Kolmogorov-Smirnov test (Table 2), and for the comparison of the means, of the Unequal Variance test (Table 3).

Short RSIs. On figure 12.A, we represent the distribution of S_{losing}, the synaptic activity at the time of the decision for the losing population, in the short RSI case

(500 ms). We find that the post-error and post-correct synaptic distributions of the losing population, as well as their means, show statistically significant differences.

RSI	Winning Population	Losing Population
500 ms	Reject, $p = 9.9 \times 10^{-8}$	Reject, $p = 5.3 \times 10^{-19}$
5000 ms	Reject, $p = 0.0044$	Reject, $p = 0.00067$

Table 2: Table of the results for the Smirnov-Kolmogorov test between the post-error / correct distributions of the synaptic activities at the time of the decision, with respect to the null hypothesis.

RSI	Winning Population	Losing Population
500 ms	Fail to reject, $p = 0.16$	Reject, $p = 2.7 \times 10^{-20}$
5000 ms	Fail to reject, $p = 0.87$	Fail to reject, $p = 0.57$

Table 3: Table of the results for Unequal Variance (Welch) test, between the post-error / correct distributions of the synaptic activities at the time of the decision, with respect to the null hypothesis.

However performing the same analysis on the the winning population gives a different result. The post-error and post-success distributions of the synaptic activities still reveal differences, but the difference in the means is not statistically significant. Hence, the difference in dynamical activities between error and correct trial is very subtle.

Long RSIs. In the case of long RSIs (Figure 12.B and D), the post-error and post-correct distributions of both populations are still different, despite a larger p-value for the Kolmogorov-Smirnov test. However, we find that the means of the synaptic activities of both the winning and the losing populations do not reveal statistically significant differences (Table 3). This is in accordance with the fact that post-error slowing vanishes at long RSI. Again, the fact that the distributions are different, but not the means, shows the subtlety of this effect.

To conclude, the synaptic distributions are different depending on the correctness of the decision, leading to a different relaxation dynamics, hence a different state at the onset of the next stimulus. This effect is stronger for the losing population, and weakens with longer RSIs.

4 Discussion

4.1 Explanations for post-error slowing

Since the fist discovery of PES in behavioral data, several cognitive explanations have been proposed.

1. The first one is called *increased response caution* (Rabbitt and Rodgers, 1977). The idea is that the response threshold would be modified, the decision becoming less cautious after a correct response and more cautious after an error.

2. The second option, called *a priori bias*, is that, after an error response, there is a bias induced by a shift in the initial state for the next trial (Rabbitt and Rodgers (1977), Laming (1979b)).

3. The third explanation, *decreased variability in bias*, is that, after an error, people are able to control more accurately the timing of the onset of information accumulation (Laming, 1979a).

4. The fourth one, called *distraction of attention*, is that the occurrence of an error is a surprising event that distracts subjects (Notebaert et al., 2009).

5. The last one, *delayed startup*, is that errors can delay the start of evidence accumulation during the next trial (Rabbitt and Rodgers, 1977).

Those explanations have been discussed in the framework of drift diffusion models (Ratcliff (1978), Dutilh et al. (2011)). Dutilh et al. (2011) qualify the hypothesis of *increased response caution* as the most likely effect, without excluding other mechanisms, notably the *a priori bias* origin. In any case, the neural correlates of increased response caution remain quite obscure, specially when the subject does not receive an external feedback on his trial. The second hypothesis, the change in *a priori bias*, can be understood as resulting from a shift in the starting point of the drift diffusion model. This explanation is in accordance with our results in the framework of attractor networks. Indeed, when performing the sequential decision-making, the dynamical analysis shows that the relaxation period, hence the state reached when the next stimulus is presented, is different following an error or a correct response. Within this dynamical picture, the shift in the initial state is intrinsically linked to the dynamical properties of the network. It is thus a robust artifact: it will occur whatever the values of the model parameters, only its amplitude will depend (and thus will or will not be measurable) on the parameters values.

4.2 Working memory and Decision-Making

In this article we have considered a specific decision-making task: the *free response time task* (Roitman and Shadlen, 2002). In such task, the subject must make a decision as soon as possible. In the different protocol called *delayed visual motion discrimination experiment* (Shadlen and Newsome, 2001), the subject must make the decision at a prescribed time after the onset of the stimulus. In such task, the decision choice must be stored in order to be retrieved at the prescribed instant of time. In the original model of attractor neural network (Wang (2002), Wong and Wang (2006)), the decision is stored as in a working memory. The persistent activity has been showed to be maintained during several seconds. The implementation of the corollary discharge that we have introduced prevents the model to show working memory effect, which is the price to pay in order to deal with successive decisions with a free response time task. A more complex model of working memory and decision-making has been studied in Murray et al. (2017). This complex architecture has two interacting modules, one implementing the working memory, the other one the decision network. It will be interesting to extend the present work by adding a working memory module in line with Murray et al. (2017), in order to obtain a network performing sequential decision-making while keeping the working memory behavior.

4.3 First and higher order sequential effects

Sequential effects can be categorized as first order (if caused by the immediately previous trial), or higher order (if caused by earlier trials in the sequence). The higher order effects of post-error trials have been described in Laming (1979b). Those sequential

effects are found to vary systematically with the RSI (Soetens et al., 1984). For short RSIs, those effects are described as automatic facilitation, and for long RSIs, they are more complicated and believed to be caused by strategic expectancy.

To account for such higher order effects, Gao et al. (2009) have introduced a dynamical network, with a network composed of four interacting modules. One is an attractor decision network based on (Usher and McClelland, 2001) (a simpler model than the one of Wong and Wang (2006), and more directly related to diffusion models than to biophysical models). The other modules includes memory units specific to alternated and repeated successive trials. This network is thus explicitly set up in such a way that it can reproduce automatic facilitation and strategic expectancy effects. In this model, even the first order effects result from a coupling between a short term memory module and the decision network. In contrast, we have shown here that our much simpler attractor network model presents these first order effects as an intrinsic property of the dynamics. In addition, it reproduces as well the post-error slowing effect (which is not studied in Gao et al. (2009)). One may ask whether a more complex architecture could account in the same way for higher order effects, that is as resulting from intrinsic properties of the dynamics, and not from an architecture with specific memory units.

Conclusion

In summary, the present work offers a biophysically motivated dynamical framework that is able to capture sequential effects in perceptual decision tasks. We have shown that an attractor neural network accounts qualitatively and quantitatively for empirical

findings about sequential and post-error effects in the absence of any specific feedback about the correctness of the decision. We have shown that these first order effects result from the intrinsic properties of the the neural dynamics.

During behavioral tasks, subjects are not always aware of their mistakes (Yeung and Summerfield, 2012), but do show post-error slowing. One may thus ask why one does not become aware that an error has been made, since the dynamics is different following an error or a success. As discussed in the paper, these differences in the dynamics are very subtle. The post-error and post-correct synaptic activities have broad distributions, with some common properties (as the same mean for example). The strong overlapping of these distributions (see Fig. 12) makes difficult to infer the correctness of the decision on a single trial basis. Yet, the tails of the post-error synaptic distribution should allow in some cases to infer that an error has been made. It would be interesting to see whether the post-error effects can be related to the confidence in one's decision (Wei and Wang, 2015; Insabato et al., 2017).

Acknowledgments

We thank Jerome Sackur and Jean-Rémy Martin for useful discussions. KB acknowledge a fellowship from the ENS Paris-Saclay.

A Appendix

A.1 Simulations and Data Analysis

Numerical simulations.

All the dynamical equations are integrated using Euler-Maruyama method in Julia language (Bezanson et al., 2014), with a time step of 0.5 ms. At the beginning of a simulation, the system is at a symmetric state, with low firing rates and synaptic activities $s_0 = 0.1$. We compute the instantaneous population firing rates, or the synaptic dynamical variables S_L and S_R, by averaging on a time window of 2 ms, slided with a time step of 1 ms. The accuracy of the network's performance is defined as the percentage of trials in which the units crossing the threshold corresponds to the stronger input. For data analysis we mainly work with the variables S_L and S_R which are analog to the firing rates of the neuron, but give less noisy figures. We consider that the system has made a decision when for the first time the firing rate of one unit crosses a threshold θ, fixed at 20 Hz. The reaction time during one trial is defined as the time needed for the network to reach the threshold from the start of the input stimulus. We neglect the possible additional time due to motor reaction.

On Figure 13 we give a schematic representation of a simulation of sequential decision-making. Each orange square corresponds to a stimulus, which last until a decision is made, with a random value of coherence in the desired range. The Julia code of the simulations can be obtained from the corresponding author on request.

We resume on Table 4 all the parameters of the simulations whose results are plotted on the figures of this article.

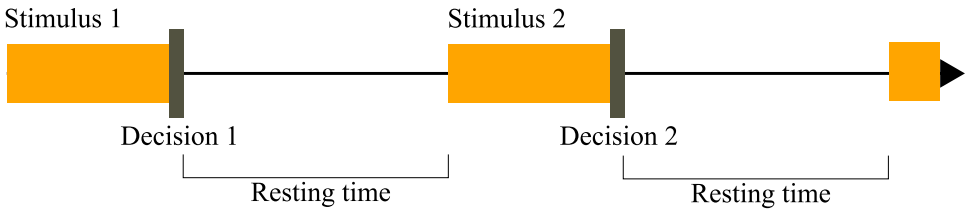

Figure 13: **Schematic diagram of the simulations.** *The time-sketch of the simulations can be decomposed into blocks. Each block is composed of: a stimulus with random specific coherence (orange), a decision associated to the end of the stimulus, a resting time with constant duration corresponding to the RSI.*

	Number of virtual subjects	Number of trials or sequences
Figure 2	1	2000
Figures 5 & 6 & 7 & 8	10	10000
Figures 9 & 10	100	5000
Figures 11 & 12	100	5000

Table 4: Simulations resume.

Statistical tests.

Following Benjamin et al. (2018), we consider a p-value of 0.005 as a criterion for rejecting the null hypothesis in a statistical test. To assess if the distributions of two variables are different, we make use of the Kolmogorov-Smirnov test (Hollander et al., 2014). For testing whether the means of two samples are different we make use of the Unequal Variance test (Welch's test) (Hollander et al., 2014).

A.2 Relaxation time constant of the dynamical network

Once the decision has been made, the system evolves in the direction of the new saddle point, whose position depends on the corollary discharge. In order to obtain some insight of the relaxation time, in the vicinity of the saddle point, we computed the eigenvalues of the saddle using the XPP software (Ermentrout and Mahajan, 2003). The relationship between time constant (τ) and eigenvalue (λ) is:

$$\lambda = \frac{1}{\tau}$$

Here, we plot on Fig. 14 the relaxation time constant of the system with respect to the strength of the corollary discharge.

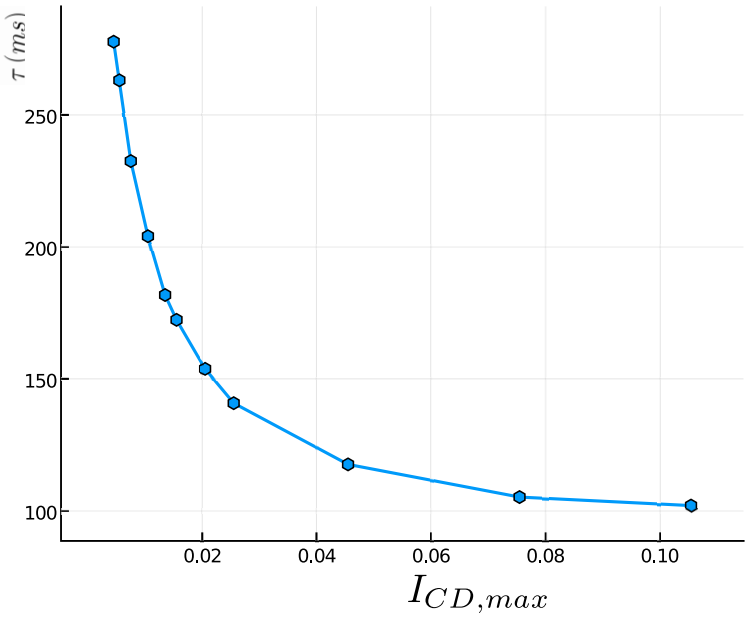

Figure 14: **Relaxation time constant.** *Relaxation time constant of the system during the RSI (that is the relaxation dynamics towards the neutral attractor state), with respect to the corollary discharge which is applied. The values are obtained by computing the eigenvalues of the dynamical system.*

References

Ashby, F. (1983). A biased random walk model for two choice reaction times. *Journal of Mathematical Psychology*, 27(3):277–297.

Benjamin, D. J., Berger, J. O., Johannesson, M., Nosek, B. A., Wagenmakers, E.-J., Berk, R., Bollen, K. A., Brembs, B., Brown, L., Camerer, C., Cesarini, D., Chambers, C. D., Clyde, M., Cook, T. D., De Boeck, P., Dienes, Z., Dreber, A., Easwaran, K., Efferson, C., Fehr, E., Fidler, F., Field, A. P., Forster, M., George, E. I., Gonzalez, R., Goodman, S., Green, E., Green, D. P., Greenwald, A. G., Hadfield, J. D., Hedges, L. V., Held, L., Hua Ho, T., Hoijtink, H., Hruschka, D. J., Imai, K., Imbens, G., Ioannidis, J. P. A., Jeon, M., Jones, J. H., Kirchler, M., Laibson, D., List, J., Little, R., Lupia, A., Machery, E., Maxwell, S. E., McCarthy, M., Moore, D. A., Morgan, S. L., Munafó, M., Nakagawa, S., Nyhan, B., Parker, T. H., Pericchi, L., Perugini, M., Rouder, J., Rousseau, J., Savalei, V., Schönbrodt, F. D., Sellke, T., Sinclair, B., Tingley, D., Van Zandt, T., Vazire, S., Watts, D. J., Winship, C., Wolpert, R. L., Xie, Y., Young, C., Zinman, J., and Johnson, V. E. (2018). Redefine statistical significance. *Nature Human Behaviour*, 2:6–10.

Bezanson, J., Edelman, A., Karpinski, S., and Shah, V. B. (2014). Julia: A Fresh Approach to Numerical Computing. *SIAM REVIEW*, 59(1):65–98.

Bogacz, R. (2009). Optimal decision-making theories. In Dreher, J.-C. and Tremblay, L., editors, *Handbook of reward and decision making*, pages 373–397. Elsevier.

Bonaiuto, J. J., De Berker, A., and Bestmann, S. (2016). Response repetition biases in

human perceptual decisions are explained by activity decay in competitive attractor models. *eLife*, 5:e20047.

Busemayer, J. R. and Townsend, J. T. (1993). Decision field theory: A dynamics-cognitive approach to desion making in an uncertain environment. *Psychological Review*, 100(3):432–459.

Dutilh, G., Vandekerckhove, J., Forstmann, B. U., Keuleers, E., Brysbaert, M., and Wagenmakers, E.-J. (2011). Testing theories of post-error slowing. *Attention, Perception, & Psychophysics*, 74(2):454–465.

Ermentrout, G. B. and Mahajan, A. (2003). *Simulating, Analyzing, and Animating Dynamical Systems: A Guide to XPPAUT for Researchers and Students*, volume 56.

Fecteau, J. H. and Munoz, D. P. (2003). Exploring the consequences of the previous trial. *Nature Reviews Neuroscience*, 4(6):435–443.

Finkel, A. S. and Redman, S. J. (1983). The synaptic current evoked in cat spinal motoneurones by impulses in single group 1a axons. *The Journal of Physiology*, 342(1):615–632.

Gao, J., Wong-Lin, K., Holmes, P., Simen, P., and Cohen, J. D. (2009). Sequential effects in two-choice reaction time tasks: decomposition and synthesis of mechanisms. *Neural computation*, 21(9):2407–36.

Gupta, P. and Cohen, N. J. (2002). Theoretical and computational analysis of skill learning, repetition priming, and procedural memory. *Psychological Review*, 109(2):401–448.

Hollander, M., Wolfe, D. A., and Chicken, E. (2014). *Nonparametric statistical methods.*, volume 2. Wiley Series in Probability and Statistics.

Insabato, A., Pannunzi, M., and Deco, G. (2017). Multiple Choice Neurodynamical Model of the Uncertain Option Task. *PLoS Computational Biology*, 13(1).

Keuleers, E. and Brysbaert, M. (2010). Wuggy: A multilingual pseudoword generator. *Behavior Research Methods*, 42(3):627–633.

Laming, D. (1979a). Autocorrelation of choice-reaction times. *Acta Psychologica*, 43(5):381–412.

Laming, D. (1979b). Choice reaction performance following an error. *Acta Psychologica*, 43(3):199–224.

Link, S. W. and Heath, R. A. (1975). A sequential theory of psychological discrimination. *Psychometrika*, 40(1):77–105.

Lo, C.-C. C. and Wang, X.-J. J. (2006). Corticobasal ganglia circuit mechanism for a decision threshold in reaction time tasks. *Nature Neuroscience*, 9(7):956–963.

McPeek, R. M., Skavenski, A. A., and Nakayama, K. (2000). Concurrent processing of saccades in visual search. *Vision Research*, 40(18):2499–2516.

Murray, J. D., Jaramillo, J., and Wang, X.-J. (2017). Working memory and decision making in a fronto-parietal circuit model. *The Journal of Neuroscience*, 37(50):12167–12186.

Notebaert, W., Houtman, F., Opstal, F. V., Gevers, W., Fias, W., and Verguts, T. (2009). Post-error slowing: An orienting account. *Cognition*, 111(2):275–279.

Pratte, M. S., Rouder, J. N., Morey, R. D., and Feng, C. (2010). Exploring the differences in distributional properties between Stroop and Simon effects using delta plots. *Attention, Perception, and Psychophysics*, 72(7):2013–2025.

Quick, R. F. (1974). A vector-magnitude model of contrast detection. *Kybernetik*, 16(2):65–67.

Rabbitt, P. and Rodgers, B. (1977). What does a man do after he makes an error? an analysis of response programming. *Quarterly Journal of Experimental Psychology*, 29(4):727–743.

Ratcliff, R. (1978). A theory of memory retrieval. *Psychological Review*, 85(2):59–108.

Ratcliff, R. (2004). A Comparison of Sequential Sampling Models for Two-Choice Reaction Time Roger Ratcliff Northwestern University Philip L . Smith University of Melbourne. *Psychological Review*, 111(2):333–367.

Ratcliff, R. and McKoon, G. (2008). The Diffusion Decision Model: Theory and Data for Two-Choice Decision Tasks. *Neural Computation*, 20(4):873–922.

Roitman, J. D. and Shadlen, M. N. (2002). Response of neurons in the lateral intraparietal area during a combined visual discrimination reaction time task. *Journal of Neuroscience*, 22(21):9475–9489.

Shadlen, M. N., Hanks, T. D., Churchland, A. K., Kiani, R., and Yang, T. (2006). The Speed and Accuracy of a Simple Perceptual Decision: A Mathematical Primer. *Bayesian Brain: Probabilistic Approaches to Neural Coding*, pages 207–233.

Shadlen, M. N. and Newsome, W. T. (1996). Motion perception: seeing and deciding. *Proceedings of the National Academy of Sciences of the United States of America*, 93(January):628–633.

Shadlen, N. N. and Newsome, W. T. (2001). Neural basis of a perceptual decision in the parietal cortex (area lip) of the rhesus monkey. *Journal of Neurophysiology*, 86:1916–1936.

Snodgrass, J. G., Luce, R. D., and Galanter, E. (1967). Some Experiments on Simple and Choice Reaction Time. *Journal of Experimental Psychology*, 75(1):1–17.

Soetens, E., Deboeck, M., and Hueting, J. (1984). Automatic aftereffects in two-choice reaction time: A mathematical representation of some concepts. *Journal of Experimental Psychology: Human Perception and Performance*, 10(4):581–598.

Speckman, P. L., Rouder, J. N., Morey, R. D., and Pratte, M. S. (2008). Delta Plots and Coherent Distribution Ordering. *The American Statistician*, 62(3):262–266.

Tipper, S. P. (2001). Does negative priming reflect inhibitory mechanisms? A review and integration of conflicting views. *Quarterly Journal of Experimental Psychology Section A: Human Experimental Psychology*, 54(2):321–343.

Townsend, J. T. and Ashby, F. G. (1983). *The stochastic modeling of elementary psychological processes*. CAMBRIDGE UNIVERSITY PRESS.

Uchida, N. and Mainen, Z. F. (2003). Speed and accuracy of olfactory discrimination in the rat. *Nature Neuroscience*, 6(11):1224–1229.

Usher, M. and McClelland, J. L. (2001). The time course of perceptual choice: The leaky, competing accumulator model. *Psychological Review*, 108(3):550–592.

Vickers, D. (1979). *Decision processes in Visual Perception*. Academic Press.

Wang, X.-J. J. (2002). Probabilistic decision making by slow reverberation in cortical circuits. *Neuron*, 36(5):955–968.

Wei, W., Rubin, J. E., and Wang, X.-J. (2015). Role of the Indirect Pathway of the Basal Ganglia in Perceptual Decision Making. *Journal of Neuroscience*, 35(9):4052–4064.

Wei, Z. and Wang, X.-J. (2015). Confidence estimation as a stochastic process in a neurodynamical system of decision making. *Journal of Neurophysiology*, 114(1):99–113.

Wong, K.-F. and Wang, X.-J. (2006). A Recurrent Network Mechanism of Time Integration in Perceptual Decisions. *Journal of Neuroscience*, 26(4):1314–1328.

Yeung, N. and Summerfield, C. (2012). Metacognition in human decision-making: confidence and error monitoring. *Philosophical Transactions of the Royal Society B: Biological Sciences*, 367(1594):1310–1321.